Int. J. Electrochem. Sci., 14 **(2019)** 11509 – 11517, doi: 10.20964/2019.12.31

International Journal of ELECTROCHEMICAL SCIENCE
www.electrochemsci.org

Effects of nanosized Bi_2O_3 addition on the superconducting properties of $Bi_{1.6}Pb_{0.4}Sr_2Ca_2Cu_3O_{10}$

Nabil A. A. Yahya[1], *R. Abd-Shukor*[2,*]

[1] Department of Physics, Thamar University, Thamar, Yemen
[2] School of Applied Physics, Universiti Kebangsaan Malaysia, 43600 Bangi, Selangor Malaysia
[*]E-mail: ras@ukm.edu.my

Received: 2 July 2019 / *Accepted:* 29 August 2019 / *Published:* 29 October 2019

The effects of nanosized Bi_2O_3 (150 nm) addition on $Bi_{1.6}Pb_{0.4}Sr_2Ca_2Cu_3O_{10}$ ((Bi,Pb)-2223) superconductor have been investigated. Samples with nominal starting composition (Bi,Pb)-2223)$(Bi_2O_3)_x$ with x = 0-0.15 wt.% were prepared using the co-precipitation method. The structure and microstructure were examined by using powder X-ray diffraction (XRD) method and scanning electron microscopy (SEM), respectively. The onset-temperature ($T_{c\text{-onset}}$), zero-resistance-temperature ($T_{c\text{-zero}}$), and transport critical current density (J_c) were determined by using the four-probe technique. The XRD patterns confirmed the presence of Bi,Pb-2223 phase. J_c of all Bi_2O_3 added samples were higher than the non-added sample. The highest J_c, $T_{c\text{-zero}}$ and hole concentration (p) was observed in the x = 0.01 sample. At 77 K, J_c of x = 0.01 wt. % was about 42 times higher than the non-added sample. This could be due to the enhanced flux pinning as the size of Bi_2O_3 was between the coherence length and penetration depth of (Bi,Pb)-2223.

Keywords: nanosized Bi_2O_3; flux pinning centers; transport critical current density

1. INTRODUCTION

The $Bi_{1.6}Pb_{0.4}Sr_2Ca_2Cu_3O_{10}$ ((Bi,Pb)-2223) high-T_c superconductor is one of the most promising materials for applications as tapes or wires. However, the transport critical current density (J_c) is strongly suppressed by weak links and weak pinning of magnetic flux lines [1-3]. The coherence length (ξ), penetration depth (λ) and magnetic flux size in a superconductor is in the nanometer range. The weak pinning of magnetic flux lines decreases J_c with increasing temperature and magnetic field, due to the motion of the vortices.

The penetration depth, λ of (Bi,Pb)-2223 superconductor is about 1000 nm and the coherence length ξ is 2.9 nm. It is expected that the interaction between the pinning center (e.g. nanoparticles) and magnetic flux lines will be strong for a particle with size d where $\xi < d < \lambda$ [4]. The introduction of nanosized particles as defects into (Bi,Pb)-2223 can be an effective method to improve flux pinning without destroying the superconductivity and thus enhance J_c [e.g. 5,6]. The size and type of nanoparticles as the magnetic flux pinning center in $YBa_2Cu_3O_7$ and (Bi,Pb)-2223 are important parameters [7-13]. In a previous study, we have investigated the effect of nanosized PbO (10 – 30 nm) on J_c of $Bi_{1.6}Pb_{0.4}Sr_2Ca_2Cu_3O_{10}$ tapes [5].

Bismuth oxide has been useful in enhancing the superconducting properties of the cuprates such as the bismuth- and thallium-based high temperature superconductors. When Bi_2O_3 (50-80 nm) was added to (Bi,Pb)-2223, the samples with composition (Bi,Pb)-2223$(Bi_2O_3)_{0.06}$ showed the highest J_c [14]. It would be interesting to investigate the effects of Bi_2O_3 with other size on the (Bi,Pb)-2223 phase. In this work, Bi_2O_3 with size 150 nm was added into (Bi,Pb)-2223. This size was chosen because it is between ξ and λ. The onset temperature $T_{c\text{-onset}}$, zero resistance temperature $T_{c\text{-zero}}$ and J_c of (Bi,Pb)-2223$(Bi_2O_3)_x$ for x = 0 to 0.15 wt. % were measured. The structural and microstructural properties of (Bi, Pb)-2223 were also investigated.

2. EXPERIMENTAL DETAILS

The pellets were prepared from high purity powders (> 99%) of $Bi(CH_3CO_2)_3$, $Pb(CH_3CO_2).3H_2O$, $Sr(CH_3CO_2).1/2H_2O$, $Ca(CH_3CO_2).H_2O$, and $Cu(CH_3CO_2).H_2O$ with nominal starting composition $Bi_{1.6}Pb_{0.4}Sr_2Ca_2Cu_3O_{10}$. The powders were prepared by the acetate co-precipitation technique, where the filtered precipitate was calcined in a tube furnace for 12 h at 730 ºC to remove the volatile materials. An additional calcination was performed for 24 h at 845 ºC to start the formation of (Bi,Pb)-2223 superconducting phase. The size of the precursor powder was a few micrometers. Bi_2O_3 with size 150 nm (US-nano, 99+% purity) was added into (Bi,Pb)-2223 with different concentrations (x = 0, 0.01, 0.05, 0.01 and 0.15 wt.%). The mixed powders were ground and then pressed into pellets of ~ 12 mm diameter and ~ 2 mm thickness and sintered for 48 h at 845 ºC. The heating and cooling rate was 2 °C/min.

The phase and structure of the samples were examined by a D8 Advance X-ray diffractometer (XRD) from Bruker AXS with a CuK_α source (λ = 0.15406 nm). The volume fraction of Bi-2223 (high-T_c phase) and Bi-2212 (low-T_c phase) was estimated from the total intensities of these phases using the following equations [15,16]:

$$\text{Bi-2223 \%} = \frac{\sum I_{2223}}{\sum I_{2223} + \sum I_{2212}} \times 100\%$$

$$\text{Bi-2212 \%} = \frac{\sum I_{2212}}{\sum I_{2223} + \sum I_{2212}} \times 100\%$$

The microstructure of the samples was recorded using a Zeis VPSEM (Leo 1450). The size of Bi_2O_3 was determined by transmission electron microscope (HRTEM, JEOL JEM- 2100F). The four-probe technique was used to determine $T_{c\text{-onset}}$ and $T_{c\text{-zero}}$ of the pellets. The effect of nanosized Bi_2O_3

on J_c was determined by using four-probe technique from 30 to 77 K in self-fields. The 1-μV/cm criterion was used to determine J_c.

3. RESULTS AND DISCUSSION

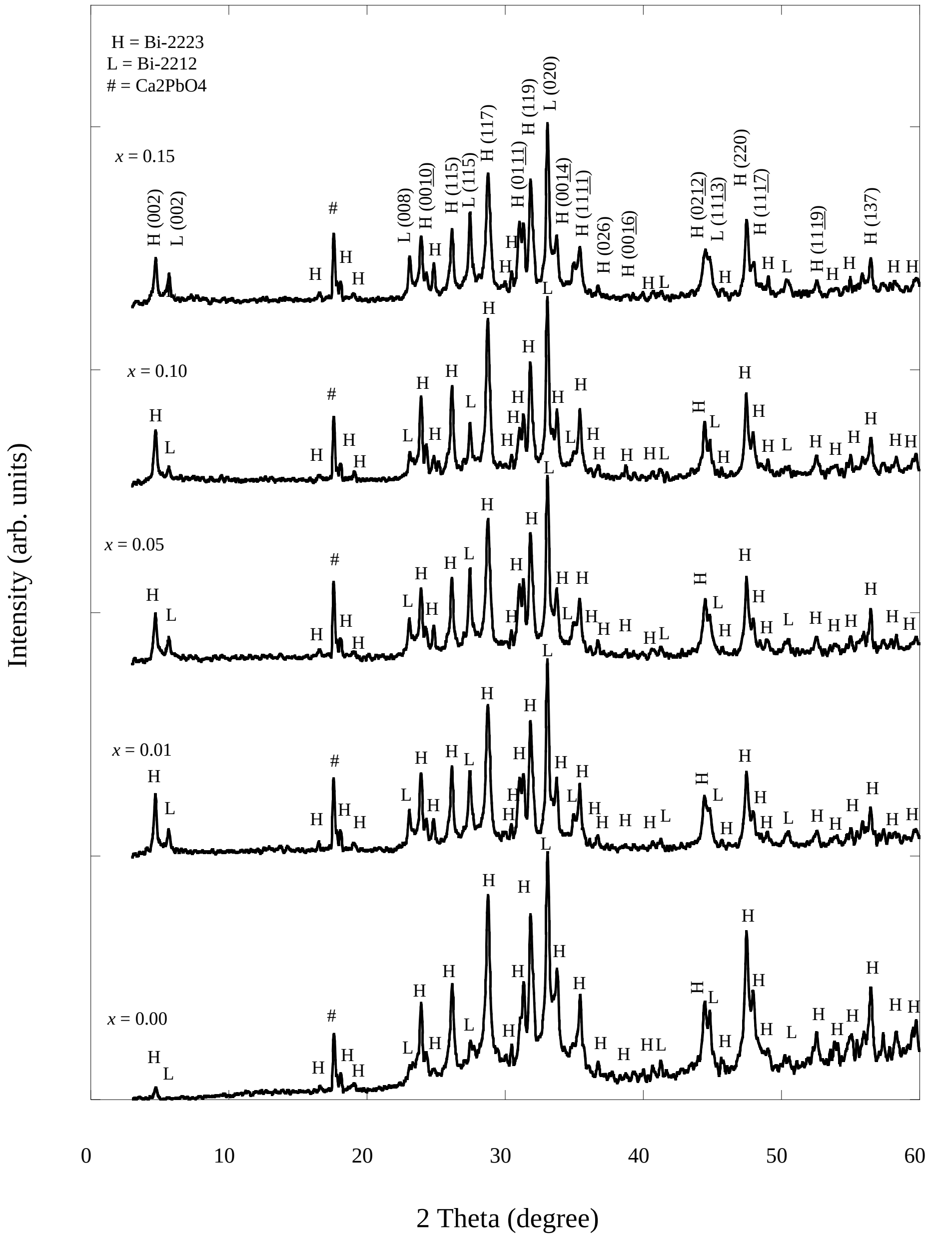

Figure 1. XRD patterns of (Bi,Pb)-2223$(Bi_2O_3)_x$ for x = 0, 0.01, 0.05, 0.10, and 0.15 wt. %. (*H*) indicates the high-T_c phase and (*L*) indicates the low-T_c phase

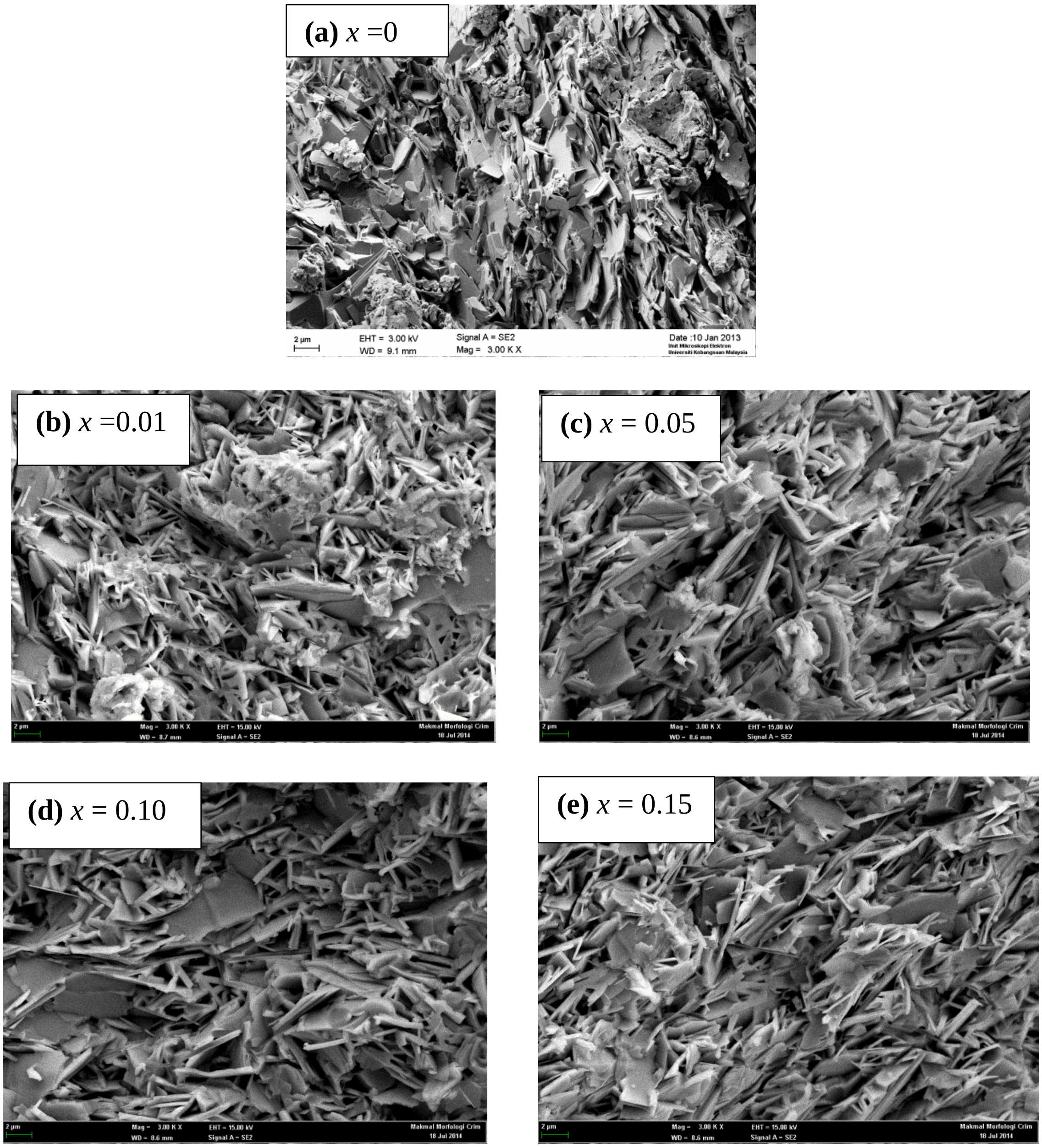

Figure 2. SEM micrographs of (Bi,Pb)-2223(Bi_2O_3)$_x$; (a) x = 0 wt. %, (b) x = 0.01 wt. %, (c) x = 0.05 wt. %., (d) x = 0.10 wt. %., and (e) x = 0.15 wt. %

Figure 1 shows the XRD patterns of (Bi,Pb)-2223(Bi_2O_3)$_x$ for x = 0, 0.01, 0.05, 0.01, and 0.15 wt.%. The XRD patterns showed that a small amount of nanosized Bi_2O_3 did not hinder the formation of (Bi, Pb)-2223 phase. Most of the peaks corresponded mainly to the Bi-2223 (high-T_c phase). Minor peaks due to the Bi-2212 (low-T_c) phase was also present in the samples. In addition, a small peak signifying the Ca_2PbO_4 phase was observed at $2\theta \approx 17.6^o$ in all samples. The lattice parameters *a, b,* and *c* of the non-added sample are 5.415, 5.407, and 37.12 Å, respectively. The lattice parameters in Bi_2O_3 added samples were almost the same as those of the non-added sample. It is therefore likely that a small amount of nanosized Bi_2O_3 did not affect the (Bi,Pb)-2223 crystal structure. SEM micrographs for (Bi, Pb)-2223(Bi_2O_3)$_x$ (x = 0, 0.01, 0.05, 0.01, and 0.15 wt.%) are shown in Figures 2(a-e). SEM of all the samples showed plate-like grain structure of the high-T_c phase (Bi-2223).

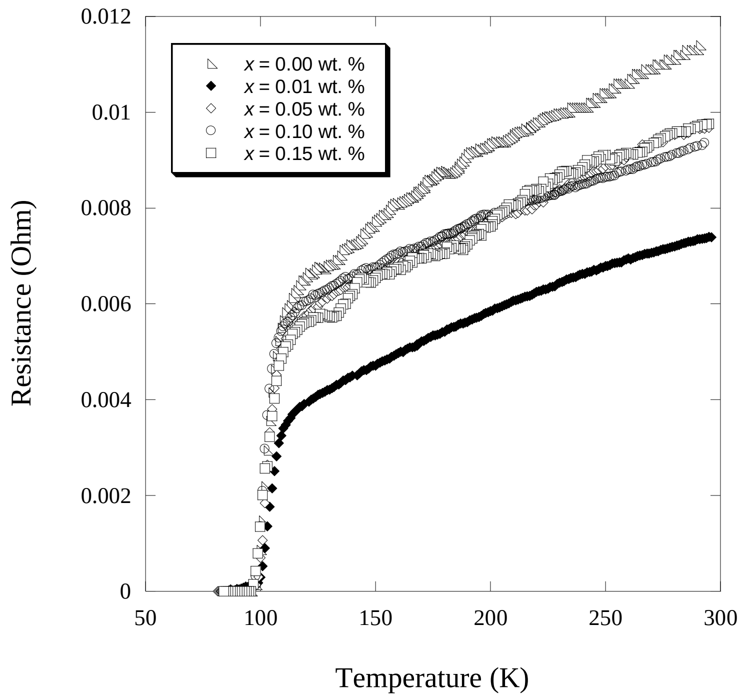

Figure 3. Temperature dependence of electrical resistance of (Bi, Pb)-2223(Bi_2O_3)$_x$ for x = 0, 0.01, 0.05, 0.10, and 0.15 wt. %

The temperature dependence of electrical resistance for all samples exhibited metallic normal state behavior (Figure 3). $T_{c\text{-onset}}$ and $T_{c\text{-zero}}$ for the non-added sample is 110 K and 98 K, respectively. The sample with x = 0.01 wt. % showed the highest $T_{c\text{-zero}}$ (99 K) among the samples and the same $T_{c\text{-onset}}$ compared with non-added sample (Table 1). It is probable that very small addition of nanosized Bi_2O_3 (x = 0.01 wt. %) slightly improved the intergranular links[17].

Table 1. Lattice parameters, volume fraction, $T_{c\text{-onset}}$, $T_{c\text{-zero}}$ J_c, (at 30 and 77 K) and hole concentration (p) of (Bi,Pb)-2223(Bi_2O_3)$_x$ for x = 0 - 0.15 wt. %

x	a / Å	b / Å	c /Å	BiPb-2223 / %	BiPb-2212 / %	$T_{c\text{-onset}}$ / K	$T_{c\text{-zero}}$ / K	p hole conc.	J_c (30 K) /mA cm^{-2}	J_c (77 K) /mA cm^{-2}
0.00	5.415	5.407	37.12	74	26	110	98	0.15934	344±10	59±2
0.01	5.403	5.417	37.11	72	28	110	99	0.15939	4620±90	2500±50
0.05	5.416	5.409	37.11	71	29	109	98	0.15934	2310±70	1640±50
0.10	5.414	5.409	37.12	74	26	108	97	0.15928	2250±40	1020±20
0.15	5.413	5.411	37.10	71	29	108	97	0.15928	1840±60	690±20

The charge carriers, *p* (hole concentration) in the samples can be calculated according to the following equation [16, 18]:

$$p = 0.16 - \left(\frac{\left(1 - T_c / T_c^{\max}\right)}{82.6} \right)^{1/2}$$

where T_c^{max} for (Bi, Pb)-2223 superconductor was taken at 110 K.

The Bi_2O_3 content dependence of hole concentration, *p*, $T_{c\text{-onset}}$ and $T_{c\text{-zero}}$ are shown in Figure 4. The hole concentration, *p* for *x* = 0.01 wt. % sample showed the highest value. The *x* = 0.05 wt. % sample showed similar hole concentration, *p* compared to the non-added sample. The hole concentration, $T_{c\text{-onset}}$ and $T_{c\text{-zero}}$ for *x* > 0.05 wt. % samples were slightly lower than those of the non-added sample. It is clear that $T_{c\text{-onset}}$ and $T_{c\text{-zero}}$ with *x* > 0.05 wt. % decreased slightly due to the decrease of the hole concentration, *p*.

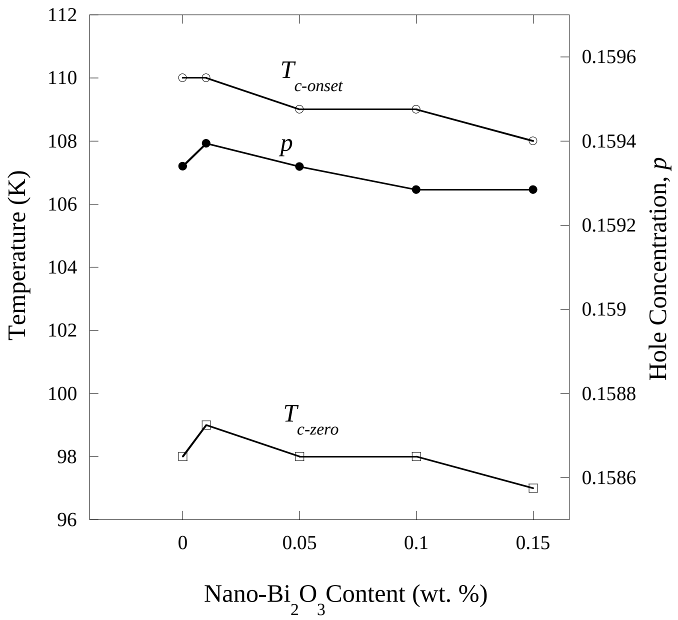

Figure 4. Nanosized Bi_2O_3 content dependence of hole concentration (*p*), $T_{c\text{-onset}}$ and $T_{c\text{-zero}}$ for *x* = 0, 0.01, 0.05, 0.10, and 0.15 wt. %

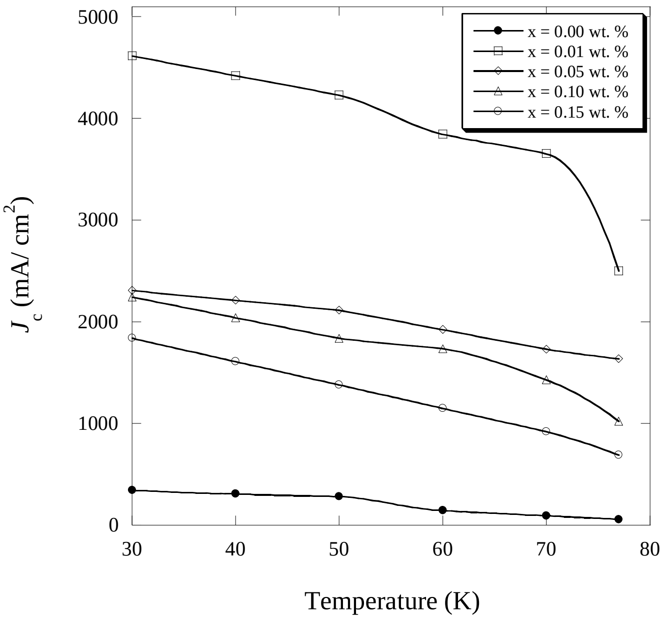

Figure 5. J_c of (Bi,Pb)-2223$(Bi_2O_3)_x$ as a function of temperature for x = 0, 0.01, 0.05, 0.10, and 0.15 wt. %

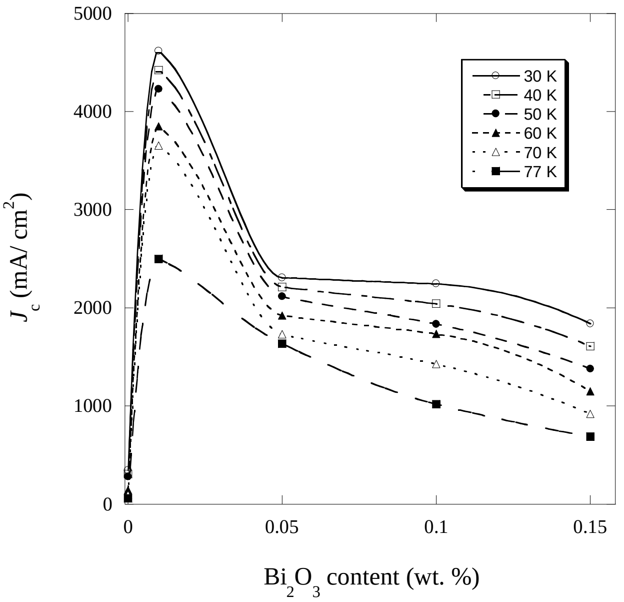

Figure 6. J_c of (Bi,Pb)-2223$(Bi_2O_3)_x$ as a function of different adding concentrations for x = 0, 0.01, 0.05, 0.10, and 0.15 wt. %

J_c for all samples as a function of temperature is shown in Figure 5. In general, J_c decreased with the increased of temperature from 30 to 77 K due to the thermally activated flux creep. All of the Bi_2O_3 added samples showed much higher J_c compared with the non-added sample. For the non-added sample, J_c at 30 and 77 K was 344 mA/cm^2 and 59 mA/cm^2, respectively. The x = 0.01 wt. % sample showed the highest J_c, which was 4615 mA/cm^2 and 2500 mA/cm^2 at 30 and 77 K, respectively. The improved J_c may be due to the enhancement of flux pinning strength as a result of nanosized Bi_2O_3 at the grain boundaries.

J_c showed a sudden decrease when the amount of Bi_2O_3 was increased to more than x = 0.01 wt. % (Figure 6). The lattice parameters, hole concentration, p, $T_{c\text{-onset}}$, $T_{c\text{-zero}}$, and J_c at 30 and 77 K of the samples are summarized in Table 1. It is interesting to note that nano PbO addition also increased J_c of the BiPb-2223 superconductor [5]. Hence, although these two elements are already in the parent compound, addition of nanosized Bi_2O_3 and PbO led to the enhancement of J_c without suppressing the transition temperature. The enhancement of J_c is possibly due to enhanced grain connectivity as a result of nanosized Bi_2O_3 at the grain boundaries. Smaller Bi_2O_3 (50-80 nm) addition showed x = 0.06 wt. % as the highest J_c value [14]. In this work, 150 nm Bi_2O_3 was used and a smaller amount (x = 0.01 wt. %) was sufficient to optimize J_c.

In conclusion, the effects of nanosized Bi_2O_3 addition on the superconducting properties of bulk $Bi_{1.6}Pb_{0.4}Sr_2Ca_2Cu_3O_{10}(Bi_2O_3)_x$ samples were investigated. The optimal amount which showed the highest J_c, $T_{c\text{-zero}}$, and hole concentration, p was x = 0.01 wt. %. J_c of x = 0.01 wt. % was about 13 and 42 times larger than the non-added sample at 30 and 77 K, respectively. The enhancement of J_c may be due to the fact that the particles size of Bi_2O_3 is larger than ξ and smaller than λ of (Bi, Pb)-2223, which can increase the flux pinning ability in the samples.

ACKNOWLEDGMENTS
This research was supported by the Ministry of Education, Malaysia under grant no. FRGS/1/2017/SG02/UKM and Thamar University, Thamar, Yemen.

References

1. A. Campbell, J. Evetts, *Adv. Phys.,* 50 (2001) 1249.
2. D. Larbalestier, *Science (Washington, DC, U. S.),* 274 (1996) 736.
3. D. S. Fisher, M.P.A. Fisher, D.A. Huse, *Phys. Rev. B,* 43 (1991) 130.
4. I. Lyuksyutov, D. Naugle, *Mod. Phys. Lett. B,* 13 (1999) 491.
5. N.A.A. Yahya, R. Abd-Shukor, *Ceram. Int.,* 40 (2014) 5197.
6. X. Wan, Y. Sun, W. Song, K. Wang, L. Jiang, *J.* Du, *Phys. C (Amsterdam, Neth.),* 307 (1998) 46.
7. I.P. Abu-Bakar, N.R. Mohd-Suib, K. Muhammad-Aizat, J. Nur-Akasyah, S. Radiman, R. Abd-Shukor, *Sains Malaysiana,* 46 (2017) 1971.
8. N.A.Yahya, R. Abd-Shukor, *J. Supercond. Nov. Magn.,* 27 (2014) 329.
9. E. Hannachi, Y. Slimani, F. Ben Azzouz, A. Ekicibil, *Ceram. Int*., 44 (2018) 18836.
10. Y. Slimani, E. Hannachi, A. Ekicibil, M. A. Almessiere, F. Ben Azzouz, *J. Alloys Compd*., 781 (2019) 664.
11. N.A. Yahya, A. Al-Sharabi, N.R. Mohd-Suib, W. Chiu, R. Abd-Shukor, *Ceram. Int.,* 42 (2016) 18347.

12. R. A. Al-Mohsin, A. L. Al-Otaibi, M. A. Almessiere, H. Al-badairy, Y. Slimani, F. Ben Azzouz, *J. Low Temp. Phys.,* 192 (2018) 100.
13. Y. Slimani, M. A. Almessiere, E. Hannachi, A. Baykal, A. Manikandan, M. Mumtaz, F. Ben Azzouz, *Ceram. Int.,* 45 (2019) 2621.
14. Nurul Raihan Mohd Suib, J. Nur-Akasyah, K. Muhammad Aizat, R. Abd-Shukor, *J. Phys.: Conf. Ser.,* 1083 (2016) 012045.
15. I. Karaca, O. Uzun, U. Kölemen, F. Yilmaz, O. Sahin, *J. Alloys Compd.,* 476 (2009) 486.
16. T. Çördük, O. Bilgili, K. Kocabaş, *J. Mat. Sci.: Mater. Electron.,* 28 (2017) 14689.
17. A. Aftabi, M. Mozaffari, *J. Supercond. Nov. Magn.* 28 (2015) 2337.
18. M. Mumtaz, L. Ali, I. Ahmad, *Phys. C (Amsterdam, Neth.),* 551 (2018) 19.